Deep inelastic nucleon transfer in $^{16}O+^{27}Al$ reactions at 90 and 100 MeV*

T. M. Cormier,† A. J. Lazzarini, M. A. Neuhausen, A. Sperduto, K. Van Bibber, F. Videbaek,‡
G. Young, E. B. Blum,§ L. Herreid,§ and W. Thoms§

Massachusetts Institute of Technology Department of Physics and Laboratory for Nuclear Science, Cambridge, Massachusetts 02139

(Received 18 September 1975)

Reactions induced by ^{16}O bombardment of ^{27}Al have been investigated using a time-of-flight spectrometer for $E(^{16}O) = 90$ and 100 MeV. Systematics of the angular distributions vs mass transfer and Q value suggest that frictional collisions are important in the transfer channels. The magnitude of deep inelastic cross sections and quasielastic cross sections are compared with previous fusion cross section measurements and limiting angular momenta are deduced.

[NUCLEAR REACTIONS $^{27}Al(^{16}O, M)$ for mass of $M=6$ through 22 amu, $E(^{16}O)=90$, 100 MeV, $^{27}Al(^{16}O, ^{16}O)$, $^{27}Al(^{16}O, C)$, $^{27}Al(^{16}O, N)$, $^{27}Al(^{16}O, O)$, $E(^{16}O)=100$ MeV. Measured $\sigma(E_M, \theta_M)$, Q values, total reaction cross section.]

I. INTRODUCTION

Heavy ion transfer reactions were initially interpreted to be quasielastic processes occurring for grazing collisions. Recent studies at higher energies[1] and with heavier beams[2-7] have shown that, particularly for multinucleon transfer, a substantial fraction of the reaction cross section may appear in channels with significant damping of the kinetic energy of relative motion. These deep-inelastic transfer reactions are believed to occur for impact parameters smaller than grazing when the energy is sufficiently high that the angular momemtum of these orbits exceeds the compound nucleus critical value. Deep-inelastic reactions have been observed for systems ranging from $^{84}Kr + ^{209}Bi$[6,7] to $^{16}O + Ni$[8,9] and the systematics of the angular distributions and Q values are becoming well established.

The mechanism of deep-inelastic collisions is of interest for several reasons. First, deep-inelastic collisions are intermediate between compound nucleus formation and direct reactions[10] in that the kinetic energy degrees of freedom are equilibrated while a memory of the entrance channel is maintained. As a result, the cross sections for deep-inelastic collisions may eventually be applied to determine heavy ion optical potentials corresponding to larger nuclear overlap than that which occurs in conventional direct reactions. Some sensitivity to the nuclear potential may already have been observed[10] experimentally in the striking difference between deep-inelastic reactions and fusion induced by ^{40}Ar and ^{84}Kr beams on heavy targets.

A second reason for interest in the mechanism of deep-inelastic collisions is that the nearly complete damping of the kinetic energy of relative motion which is observed is a result of nuclear viscosity. Thus it is possible that precise measurements of the systematics of optimum Q values vs mass transfer and angle may yield information on this parameter which is important from the point of view of nuclear fission theory.

Finally, because it is responsible for the decrease of compound nucleus cross sections for very heavy targets, the mechanism of deep-inelastic reactions is important in estimating cross sections for the production of superheavy nuclei.

The present work reports on the observation of deep-inelastic transfer reactions for $^{16}O + ^{27}Al$ at $E_{lab}(^{16}O) = 90$ and 100 MeV. Reaction products have been detected with a time-of-flight spectrometer, allowing us to investigate the mass transfer systematics of deep-inelastic events with unit mass resolution. Products with masses of 6 through 22 amu have been studied.

II. EXPERIMENTAL METHOD

The ^{16}O beam of 90 and 100 MeV from the upgraded BNL three-stage tandem facility was used to bombard aluminum foils of 1.0 to 1.5 mg/cm^2 thickness. Up to 2 μA of momentum analyzed beam was available. Reaction products were detected using a time-of-flight spectrometer[11] which employed a thin film plastic scintillator ($\sim 40\mu g/cm^2$) start detector and surface barrier stop detector of 300 mm^2 active area. A flight path of 1 m was used.

Energy (E) and time-of-flight (T) signals were processed using a multiplier circuit which produced a mass signal ($\sim ET^2$). Two dimensional mass-energy spectra of 256×128 channels were collected live using an on-line computer. Figure 1 shows a typical mass-energy spectrum obtained at $\theta_{lab} = 40°$ and $E(^{16}O) = 100$ MeV. Dead time and pile-up corrections were made, although the total cor-

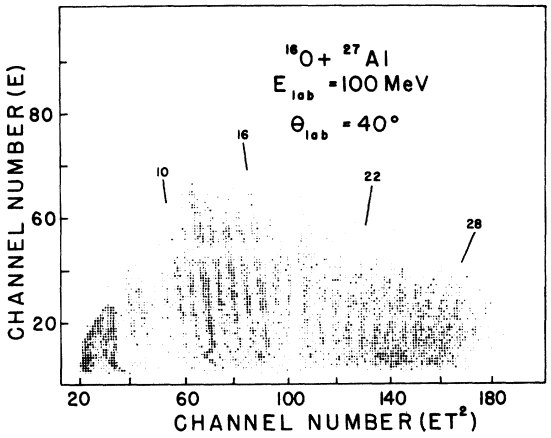

FIG. 1. Mass-energy spectrum of $^{16}O + ^{27}Al$ reaction products at $\theta_{lab} = 40°$ with $E(^{16}O) = 100$ MeV.

rection amounted to $\simeq 3\%$. Energy spectra for individual mass lines were projected and plotted as a function of Q value assuming two-body kinematics. Corrections for energy loss in the target were made using the tables of Northcliffe and Schilling.[12] An energy calibration was obtained from the ^{16}O elastic scattering and as a result no corrections could be made for the well known[13,14] mass dependence of the calibration coefficients. However, previous experience with this effect allows us to estimate that the maximum systematic error introduced will be everywhere less than 2 MeV for ion masses of 6 through 22. Some sample energy spectra obtained at $E(^{16}O) = 100$ MeV and $\theta_{lab} = 25°$ are shown in Fig. 2. Angular distributions for product masses 6 through 22 were obtained from $\theta_{lab} = 5.1°$ to 55° at $E(^{16}O) = 90$ MeV and from $\theta_{lab} = 10°$ to 65° at $E(^{16}O) = 100$ MeV. The angular resolution in both cases was ~1°.

A monitor detector placed at 30° was used to obtain a relative normalization of the angular distributions. Absolute cross sections were obtained by normalizing to the experimental differential evaporation residue cross sections of Kozub *et al.*[15] This procedure required a linear interpolation between the results of Ref. 15 obtained at $E(^{16}O) = 81$ and 105 MeV to our energies of 90 and 100 MeV. The evaporation residue cross sections interpolated from Ref. 15 are given in Table I. The largest error in this procedure arises from the uncertainty in measured lab angle ($\sim \pm 0.2°$) and this is expected to introduce a $\pm 10\%$ uncertainty in our cross sections relative to the total fusion cross sections of Ref. 15.

In an independent experiment at $E_{lab}(^{16}O) = 100$ MeV, a surface barrier detector telescope with a 7.7 μm thick first element and 500 μm thick second element was used to measure the $^{16}O + ^{27}Al$ elastic

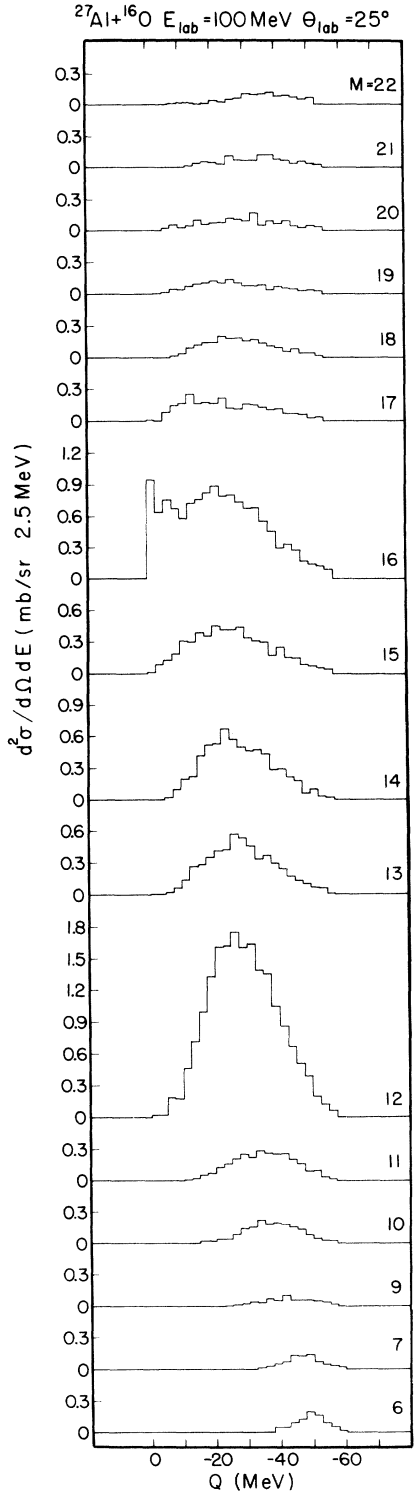

FIG. 2. Energy spectra for product masses 6 through 22 in terms of absolute cross section per 2.5 MeV Q bin versus Q value. $E(^{16}O) = 100$ MeV and $\theta_{lab} = 25°$.

TABLE I. Experimental differential cross sections for $^{16}O+^{27}Al$ evaporation residues interpolated from the results of Kozub *et al.* (Ref. 14).

$E(^{16}O)$ (MeV)	θ_{lab}	$(d\sigma/d\Omega)_{lab}$ (mb/sr)
100	15	1400± 200
90	7	4470± 300
	17	990± 50

scattering angular distribution, as well as the angular distribution of carbon, nitrogen, and oxygen reaction products. During the elastic scattering measurements, the telescope was positioned such that it subtended an angular range of 0.1° in the reaction plane. Elastic scattering measurements were made from θ_{lab} =3° to 18° in 1° steps. The absolute cross section scale was established by normalizing to Rutherford scattering at θ_{lab} = 3°. Uncertainties in the absolute cross section scale arising from misalignment of beam direction at the target, movement of the beam spot on target, and errors in angle measurements are expected to amount to ± 20%.

During the measurement of the C, N, and O angular distributions, the telescope was positioned so as to subtend ± 1° in the reaction plane. Data were obtained from θ_{lab} =20° to 75° in 5° steps.

Both the telescope and time-of-flight experiments frequently involved the detection of low energy ions. As a result, carbon contamination of the target was a major concern. To minimize this problem, targets were prepared from ultra-pure (99.999%) aluminum; and during beam exposure, the vacuum in the vicinity of the target was maintained between 1×10^{-6} and 3×10^{-7} Torr. As a check on the amount of carbon buildup that was occurring, each angle measured on an aluminum target was also measured on a 10 $\mu g/cm^2$ ^{12}C target. By this precaution, plus periodically moving the target to expose a fresh spot to the beam, we were able to keep the contamination of our spectra by products from ^{12}C to a negligible level.

III. EXPERIMENTAL RESULTS AND DISCUSSION

A. Energy spectra and mass distributions

Energy spectra for product masses 6 through 22 are shown in Fig. 2 plotted versus Q value calculated for a two-body final state. The abscissa is an absolute cross section scale. The spectra are generally bell shaped and peak at Q values ranging from ~ − 50 to − 20 MeV with widths ranging from 10 to 35 MeV. These deep-inelastic optimum Q values vary in a systematic fashion with mass transfer as discussed in Sec. III 2. One noteworthy feature of the mass 16 spectrum is the occurrence of a deep-inelastic group centered at Q = − 23 MeV which is well resolved from the elastic and quasi-elastic peaks. This deep-inelastic group is resolved at angles $\theta_{lab} \gtrsim 20°$.

To obtain a mass spectrum characteristic of the deep-inelastic transitions, we have integrated the spectra of Fig. 2 from Q = − 20 to − 50 MeV. The result is shown in Fig. 3. The most outstanding feature of this plot is the strong enhancement of mass 12 and mass 16. Measurements made with an E-ΔE Telescope have indicated that this enhancement is due primarily to ^{12}C and ^{16}O, respectively. Aside from the strong enhancement of M = 12 and 16, the mass distribution is moderately smooth and peaks near M = 13 or 14, indicating a strong enhancement of stripping relative to pickup reactions. Two explanations have been offered[3] to account for this enhancement: (i) The optimum Q values for few nucleon pickup and stripping are comparable (see Sec. III 2), while ground state Q values (Q_{gg}) for stripping are more positive by ~ 8 MeV. As a result, stripping reactions tend to populate higher excited states than do pickup reaction. Thus, due to the increased level density, the number of final states available to stripping reactions is greater than the number available to pickup channels. (ii) A second explanation for the enhancement of stripping is that it is only an apparent enhancement due to nucleon decay of the primary fragments. The magnitude of the first effect can be estimated in the present case using a standard Fermi gas level density expression with standard parameters[16] including pairing. If we assume

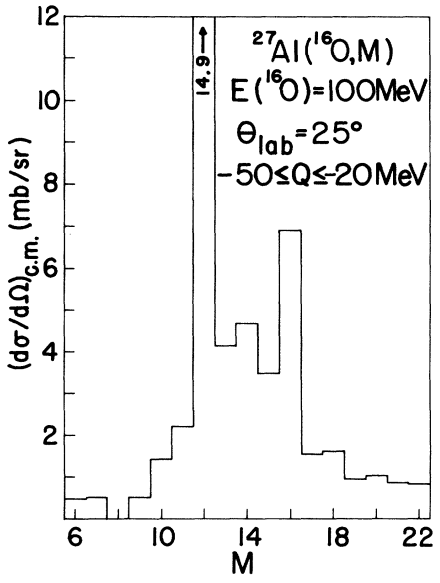

FIG. 3. Mass spectrum of all events with $-50 \leq Q \leq -20$ MeV at θ_{lab} = 25° and $E(^{16}O)$ = 100 MeV.

that $M = 15$ is predominantly ^{15}N and $M = 17$ is predominantly ^{17}O and if we assume that all of the excitation energy resides in the heavy fragment, then at the optimum Q value of -35 MeV indicated in Fig. 2, the excitation energy difference is 8.371 MeV and the level density ratio is ~3.5. This is only a factor of ~1.6 larger than the observed enhancement which indicates that the enhancement of stripping reactions is consistent with ground state Q value differences.

Also of interest in Fig. 3 is the existence of a weak but significant odd-even effect resulting in the enhancement of $M = 14$, 18, and 20 relative to neighboring masses. The only significant deviation from the enhancement of even masses is that $M = 11$ appears to be too strong. One possible explanation of the anomalously enhanced $M = 11$ group is that a significant portion of the mass 11 yield is the result of nucleon decay of $M = 12$ ions in flight. This is a reasonable assumption to make in view of the intensity of the $M = 12$ group. In fact, if we assume that the odd-even effect should persist to $M = 10$ and 11, then we can estimate that ~5–10% of the $M = 12$ ions decay by nucleon emission in flight. We should note in passing that if this crude estimate is correct, then nucleon decay of the primary fragments will not account for the observed enhancement of stripping reactions.

The odd-even effect seen here in the mass spectrum has been seen previously in z distributions of deep-inelastic events for $^{40}Ca + ^{40}Ca$,[4] and to a lesser degree in $^{40}Ar + ^{232}Th$,[2,3] and also in the N and Z distributions of $^{40}Ar + Ni$.[5] Two possibilities are frequently cited to account for the enhancement of even-A fragments: (i) The odd-even effect of the nucleon binding energies could influence the sequential decay of the primary fragments so as to favor the production of even-A secondary fragments. (ii) The production of even-A light fragments results in the production of an associated odd-A heavy fragment. Thus the production of an even-A light fragment results in a higher density of final states.

B. Deep inelastic optimum Q values

Optimum Q values (Q_{opt}) defined as the Q value corresponding to the largest center-of-mass cross section at a given angle is plotted in Fig. 4 (note the suppressed zero) as a function of mass transfer to the projectile for $\theta_{lab} = 25°$ and 40°. Also plotted is the full width at half maximum (Γ_{FWHM}) of the distributions. The shaded regions plotted in Fig. 4 are the Q values corresponding to particle energies at the Coulomb barrier for tangent spheres with $r_0 = 1.2$ to 1.4 fm and $R = r_0(A_1^{1/3} + A_2^{1/3})$. Coulomb energies are calculated assuming $Z = \frac{1}{2}A$.

The appearance of the Q_{opt} curves is easily understood. At forward angles (e.g., $\theta_{lab} = 25°$) the optimum Q value is determined by two purely kine-

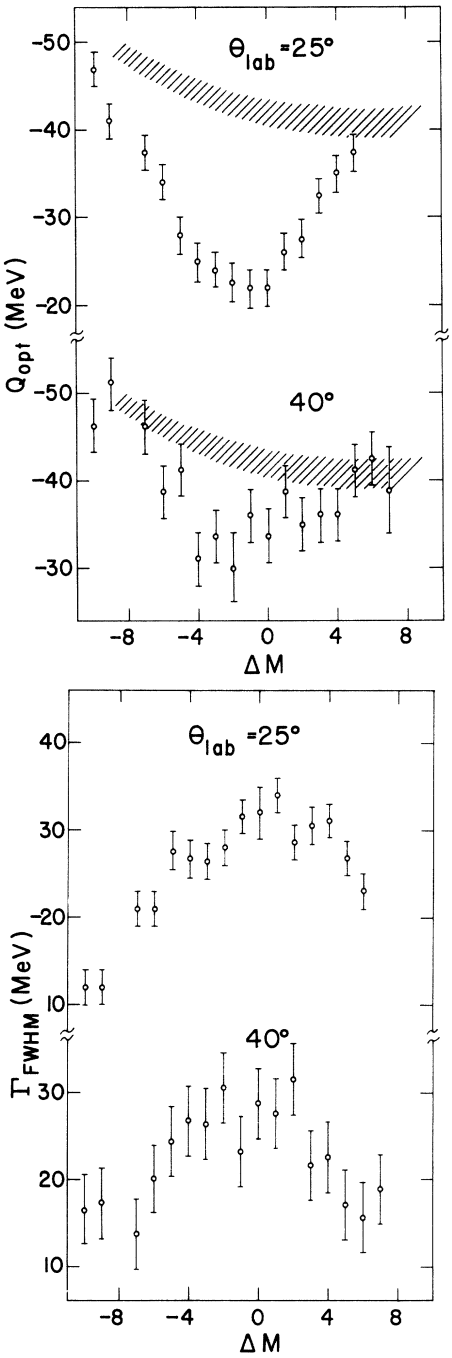

FIG. 4. Optimum Q value (Q_{opt}) and full width at half maximum (Γ_{FWHM}) of energy spectra of $\theta_{lab} = 25°$ and 40° plotted versus mass transfer to the projectile. The shaded regions are Q values corresponding to particle energy at the exit channel Coulomb barrier for $r_0 = 1.2$ to 1.4 fm.

matic factors[17]: (i) Q_{opt} should increase with the Coulomb energy in the exit channel and (ii) Q_{opt} should become more negative symmetrically for increasing mass stripping or pickup. The latter effect arises because each transferred nucleon must be accelerated to the velocity of the nucleus in which it resides in the exit channel. The fact that the first effect is a monotonic function over the range of our data while the second effect is expected to be symmetric with respect to $\Delta M = 0$ may account for the slight asymmetry of the Q_{opt} curve observed at 25°.

The optimum Q value curve vs mass transfer for $\theta_{lab} = 40°$ is more characteristic of the type expected for deep-inelastic transfer reactions. At this angle we observe an almost complete damping of the kinetic energy of relative motion. One difference between the present data and similar measurements for heavy nuclei such as $^{40}Ar + ^{232}Th$ is that in the present case, particle energies are systematically higher than the Coulomb barrier for tangent spheres, whereas for heavy systems the reverse is true. For heavy nuclei the interpretation is that the exit channel Coulomb barrier at scission is considerably reduced due to deformation and neck formation. In the present data, the observation of particle energies 5 to 10 MeV in excess of the tangent sphere Coulomb barrier may reflect a residual competition with the quasielastic process.

C. Angular distributions and total cross sections

Sample angular distributions obtained at $E(^{16}O) = 90$ and 100 MeV are shown in Figs. 5 and 6. The

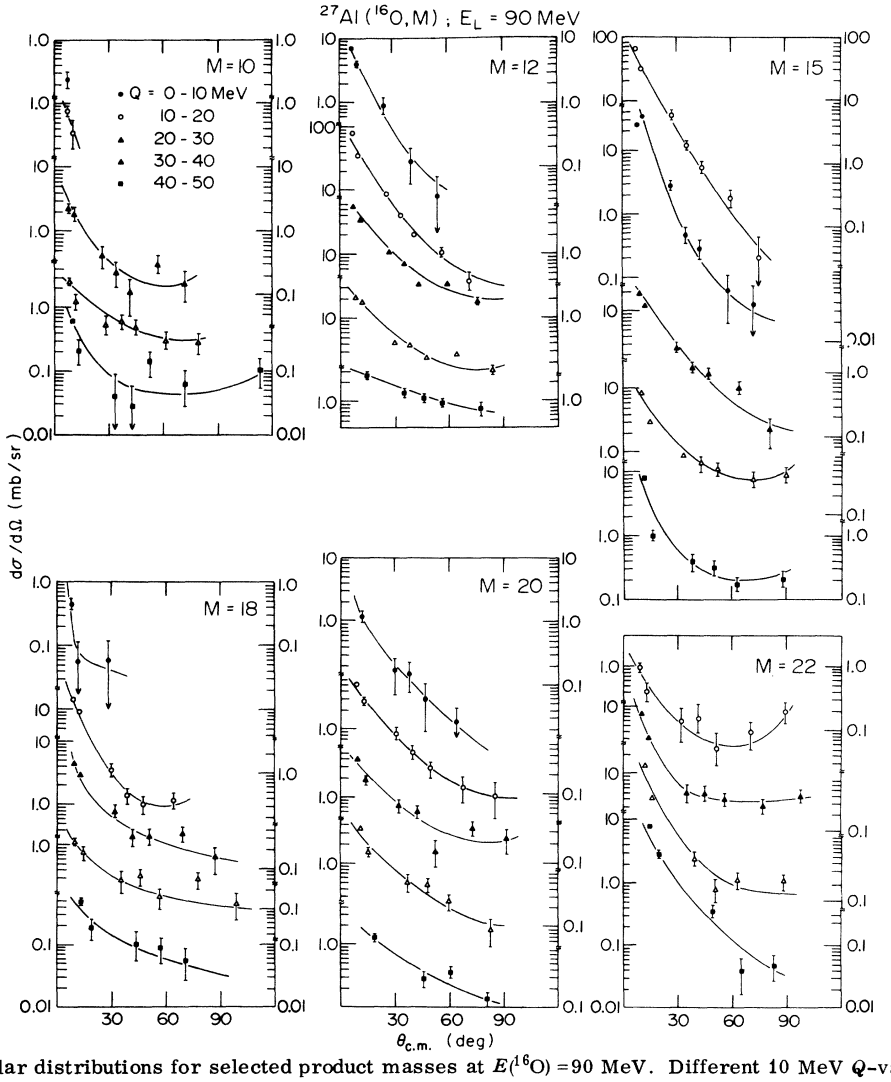

FIG. 5. Angular distributions for selected product masses at $E(^{16}O) = 90$ MeV. Different 10 MeV Q-value windows are plotted separately to illustrate the flattening of the angular distributions at large inelasticity. The solid curves are drawn to guide the eye.

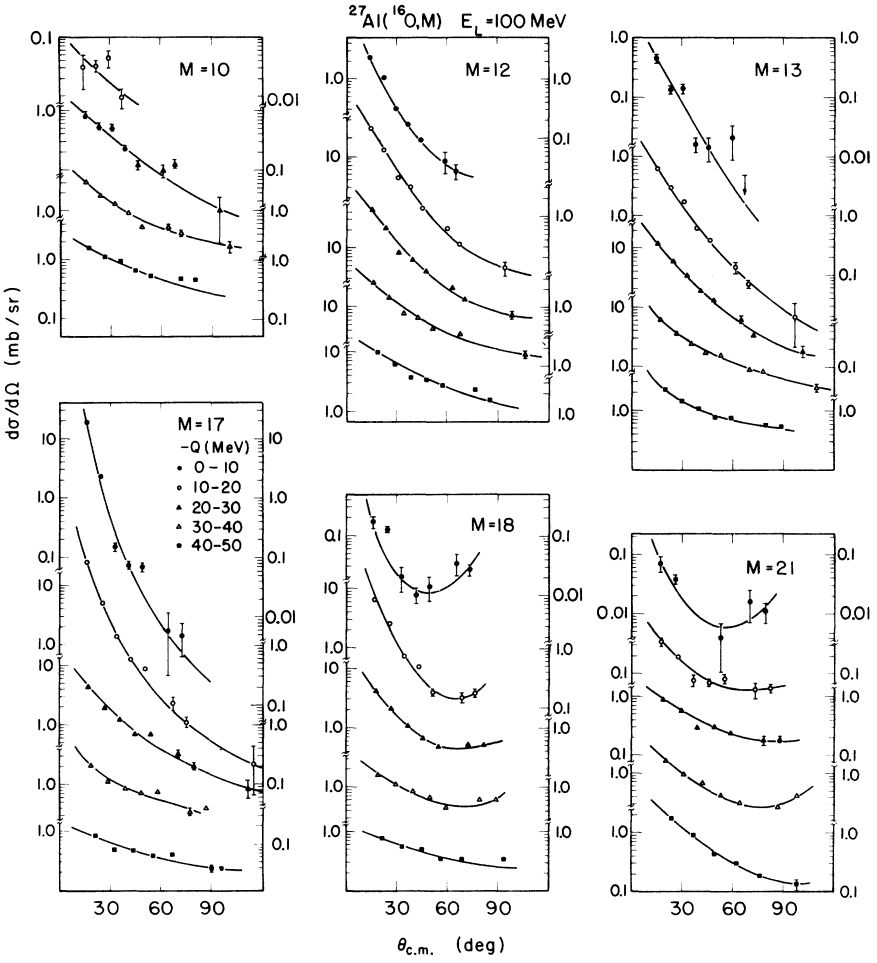

FIG. 6. Angular distributions for selected product masses at $E(^{16}O) = 100$ MeV. Different 10 MeV Q-value windows are plotted separately to illustrate the flattening of the angular distributions at large inelasticity. The solid curves are drawn to guide the eye.

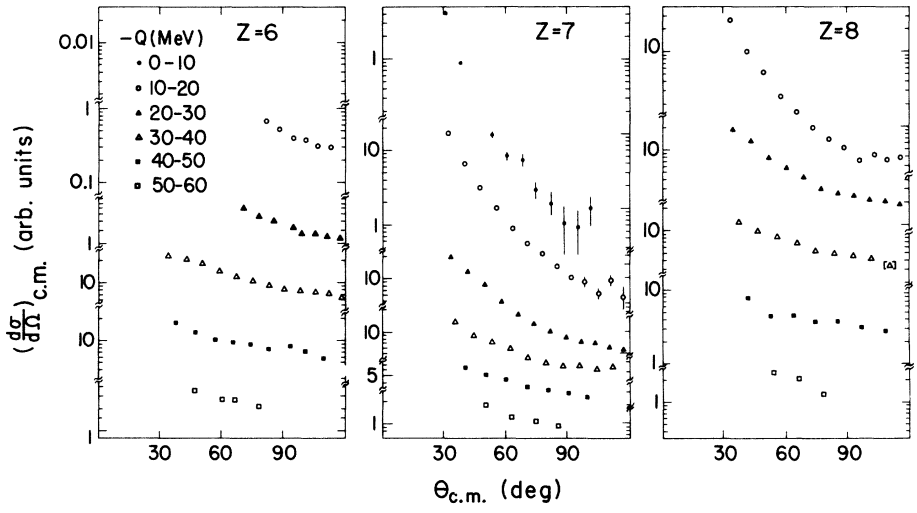

FIG. 7. Angular distributions of carbon, nitrogen, and oxygen yields at $E(^{16}O) = 100$ MeV. Different 10 MeV Q-value bins are plotted separately.

data are shown integrated over 10 MeV Q-value bins and solid lines are drawn to guide the eye. An obvious systematic trend in the data is the flattening of the angular distributions as the inelasticity increases. The effect is somewhat more pronounced at $E(^{16}O) = 100$ MeV than at 90 MeV. The systematics observed in the present case are exactly analogous to those observed by Galin *et al.*[1] for 113 MeV $^{14}N + Ag$, Artukh *et al.*[2] for $^{40}Ar + ^{232}Th$, and Albrecht *et al.*[9] for 96 MeV $^{16}O + Ni$. The phenomenon has been identified by Wilczynski[18] as the result of nuclear orbiting in frictional collisions.

Several of the angular distributions are observed to approach isotropy for $\theta_{c.m.} \simeq 90°$ and the question arises whether there is any evidence for a compound nucleus fission process. The present data do not furnish sufficient information for $\theta_{c.m.} > 90°$ to resolve the question. Figure 7 shows angular distributions for C and N and O yields obtained with the E-ΔE telescope. High energy carbon events were lost because they deposited insufficient energy in the ΔE detector. This figure supplies data for Q values expected from fission energetics (-40 to -50 MeV) for $\theta_{c.m.}$ between 90° and 120° with better statistics than were obtained in the time-of-flight measurements. The data are consistent with a monotonic decrease of cross section for $\theta_{c.m.} > 90°$ and no evidence for compound nucleus fusion-fission is seen. A reasonable upper limit for the total fusion-fission cross section at $E(^{16}O) =$ MeV is $\sigma_{fus\text{-}fiss} < 20$ mb. This number is obtained by assuming that the fission mass distribution should be symmetric and that the differential cross section observed at $\theta_{c.m.} = 90°$ is equal to the fusion-fission differential cross section. A total cross section estimate of 20 mb is obtained after assuming a $1/\sin\theta$ angular dependence. The need for better measurements is clearly indicated for $\theta_{c.m.} > 90°$ if a more accurate limit is to be set. The present experimental techniques become difficult to apply, however, in the required angular range because the particle energies become very low.

Total cross sections for all significant reactions exclusive of fusion have been determined from our angular distributions at $E(^{16}O) = 90$ and 100 MeV. For the sake of discussion, the $Q = 0$ to -20 MeV events will be termed quasielastic and the corresponding total cross section is denoted σ_{QE}. This definition of the quasielastic cross section is not completely arbitrary, since the energy spectra at angles $\theta_{lab} \leq 10°$ are characterized by a strong enhancement in the $Q = 0$ to -20 MeV window. The remaining events $Q < -20$ MeV are termed deep inelastic and the total cross section is denoted σ_{DI}. The total evaporation residue cross section is denoted σ_{ER} and the total reaction cross section is σ_R. Obviously

$$\sigma_R = \sigma_{ER} + \sigma_{DI} + \sigma_{QE} + \sigma_{fus\text{-}fiss}. \tag{1}$$

Total cross sections obtained by numerical integration of the data are displayed in Table II. Error estimates include statistical errors as well as the uncertainty in the extrapolation to 0 and 180°, but do not include the uncertainty in the absolute normalization, namely the evaporation residue cross sections of Ref. 15. The evaporation residue cross sections of Table II have been obtained by interpolation of the results of Ref. 15. The total reaction cross sections displayed in Table II were obtained from Eq. (1) ($\sigma_{fus\text{-}fiss} = 0$). In addition, for $E(^{16}O) = 100$ MeV, we have obtained σ_R from a quarter-point[19,20] analysis of the elastic scattering. The agreement obtained between the two methods is excellent.

The maximum angular momenta associated with σ_{ER} and σ_R are also given in Table II. These numbers were obtained in the sharp cutoff approximation. In this method one writes

$$\sigma_{ER} = \pi\lambda\!\!\!^{-2} \sum_{l=0}^{\infty} (2l+1) T_l, \tag{2}$$

where T_l, the absorption coefficient, is taken to be

$$T_l = \begin{cases} 1 & l \leq l_{cr} \\ 0 & l > l_{cr} \end{cases}. \tag{3}$$

Then

$$\sigma_{ER} = \pi\lambda\!\!\!^{-2}(l_{cr}+1)^2. \tag{4}$$

A similar formula is used for σ_R and corresponding cutoff angular momentum l_{max}.

TABLE II. Total cross sections and sharp cutoff l values for evaporation residues (σ_{ER}), quasielastic (σ_{QE}), and deep-inelastic (σ_{DI}) events as defined in the text.

$E(^{16}O)$ (MeV)	$E_x(^{43}Sc)$	σ_{ER} [a]	l_{cr}	σ_{DI}	Δl_{DI}	σ_{QE}	σ_R	l_R
90	69.56	1025 ± 200	29 ± 2	260 ± 50	3	170 ± 35	1455 ± 210	34^{+3}_{-2}
100	75.91	1035 ± 200	30.5 ± 3	481 ± 50	6.5	174 ± 30	1690 ± 210	39.3 ± 2.5
							1770 ± 200 [b]	40 ± 2 [b]

[a] Interpolated from the results of Ref. 15.
[b] From quarter-point analysis of elastic scattering.

Inspection of Table II reveals that the evaporation residue and quasielastic cross sections do not change between 90 and 100 MeV and that the total change in the reaction cross section of ~250 mb appears in the deep-inelastic cross section. This results in nearly doubling σ_{DI} between 90 and 100 MeV. The sixth column of Table II gives Δl_{DI}, the number of partial waves contributing to σ_{DI}, which is seen to sharply increase between 90 and 100 MeV.

As mentioned in Ref. 15, the l_{cr} for $^{16}O + ^{27}Al$ is in good agreement with the predictions of the friction model of Gross and Kalinowski[21] ($l_{cr} = 32-34$), as well as the fission competition model of Plasil and Blann[22] ($l_{cr} = 30-33$). The present results show, however, that the fission decay mode of the compound nucleus is negligible at the present energies ($\sigma_{fus-fiss} \lesssim 20$ mb). Plasil and Blann[22] calculate l_{cr} by assuming that σ_R is equal to the compound nucleus formation cross section and l_{cr} is that angular momentum which separates $\sigma_{fus-evap} = \sigma_{ER}$ from $\sigma_{fus-fiss}$. They point out, however, that compound nucleus formation may be inhibited by entrance channel conditions before the effects of fission competition are observable. The negligible compound nucleus fission yield indicates that such entrance channel conditions are operating in the present case.

IV. CONCLUSIONS

The present work has shown that there is a remarkable similarity in the systematics of deep-inelastic transfer reactions of $^{16}O + ^{27}Al$ with those of the heaviest nuclear systems. In particular, we have observed enhancement of stripping reactions, enhancement of even-A fragments, and angular distributions which approach isotropy at very negative Q values, as in studies with very heavy nuclei (e.g., $^{40}Ar + ^{232}Th$). Also, the systematics of the optimum Q values vs mass transfer observed in the present case are very similar to those observed for $^{40}Ar + ^{232}Th$.

Another interesting aspect of our results is the observed high rate of increase of the deep-inelastic cross section with energy. It is known from Ref. 15 that, at $E(^{16}O) = 168$ MeV, σ_{ER} has fallen to 860 mb. This is less than half of the anticipated reaction cross section at that energy. It will be of particular interest to see what part of the missing cross section appears as σ_{DI} and what appears as $\sigma_{fus-fiss}$.

There is indirect experimental evidence that significant fission competition will not be observed, however, up to $E(^{16}O) = 165$ MeV. Pühlhofer and Diamond[23] have studied the energy dependence of γ-ray yields of $^{16}O + ^{27}Al$ and $^{20}Ne + ^{27}Al$ up to $E(^{16}O) = 165$ MeV and $E(^{20}Ne) = 206$ MeV. Their results, based on γ-line shapes, are consistent with a strong increase in direct reaction yields above $E(^{16}O) = 100$ MeV. Although it is difficult to accurately estimate the compound nucleus-fission component from their data, they do conclude that it is probably a small fraction of the total direct reaction cross section. Thus, it would appear that up to at least $E(^{16}O) = 165$ MeV, that deep-inelastic nucleon transfer reactions will be the primary limitation to compound nucleus formation.

In addition to searching for a compound nucleus fission component at higher energies, a study of the optimum Q values versus mass transfer at higher energies could be very interesting. We have noted that in the present data at large angles the optimum Q values are such that particle energies are 5 to 10 MeV in excess of the exit channel Coulomb barrier, whereas for heavy nuclei, particle energies are usually significantly below the tangent sphere Coulomb barrier. While it is possible that this difference results from a residual competition with the quasielastic process in the present case, it is also possible to explain it in terms of differing liquid drop systematics of light and heavy nuclei. It is well known from liquid drop model calculations[24] that in the fission of light nuclei, the neck is well developed at the saddle configuration and that the passage from saddle to scission is short. As a result, most of the final translational kinetic energy of light nuclei is acquired from post-scission Coulomb repulsion. For heavy nuclei, no appreciable neck is expected at the saddle configuration and the passage from saddle to scission is long. This intrinsic difference in the fission dynamics of light and heavy nuclei could lead to a systematic variation of deep-inelastic optimum Q values relative to the tangent sphere Coulomb barrier as a function of mass of the composite system. A systematic study of Q_{opt} versus mass transfer is presently in progress for targets between ^{27}Al and ^{90}Zr.

The authors wish to acknowledge informative discussions with J. D. Garrett, A. Z. Schwarzschild, and H. E. Wegner. We are also indebted to the BNL tandem operations and support personnel for their assistance.

*Work supported in part by U. S. Energy Research and Development Administration Contract No. AT(11-1)-3069.

†Present address: Physics Department, State University of New York at Stony Brook, New York 11794.

‡On leave from Niels Bohr Institute.

§Partial support from Massachusetts Institute of Technology Undergraduate Research Opportunity Program.

[1]J. Galin, D. Guerreau, M. Lefort, J. Peter, X. Tarrago, and R. Basile, Nucl. Phys. A159, 461 (1970).

[2]A. G. Artukh, G. F. Gridnev, V. L. Mikheev, V. V. Volkov, and J. Wilczynski, Nucl. Phys. A215, 91 (1973).

[3]J. C. Jacmart, P. Colombani, H. Doubre, N. Frascaria, N. Poffe, M. Riou, J. C. Roynette, C. Stephan, and A. Weidinger, Nucl. Phys. A242, 175 (1975).

[4]P. Colombani, N. Frascaria, J. C. Jacmart, M. Riou, C. Stephen, H. Doubre, N. Poffe, and J. C. Roynette, Phys. Lett. 55B, 45 (1975).

[5]B. Gatty, D. Guerreau, M. Lefort, J. Pouthas, X. Tarrago, J. Galin, B. Cauvin, J. Girard, and H. Nifenecker, J. Phys. Lett. (Paris) 35, L117 (1974).

[6]F. Hanappe, M. Lefort, C. Ngo, J. Peter, and B. Tamain, Phys. Rev. Lett. 32, 738 (1974).

[7]K. L. Wolf, J. P. Unik, J. R. Huizenga, J. Birkelund, H. Freisleben, and V. E. Viola, Phys. Rev. Lett. 33, 1105 (1974).

[8]J. Wilczynski, K. Siwek-Wilczynska, J. S. Larsen, J. C. Acquadro, and P. R. Christensen, Nucl. Phys. A244, 147 (1975).

[9]R. Albrecht, W. Dunnweber, G. Graw, H. Ho, S. G. Steadman, and J. P. Wurm, Phys. Rev. Lett. 34, 1400 (1975).

[10]J. R. Huizenga, Selected Aspects of Very Heavy Ion Reactions, series of lectures presented at the VII Summer School of Nuclear Physics, Institute of Nuclear Research, Warsaw, Poland (unpublished).

[11]T. M. Cormier, R. S. Galik, E. R. Cosman, and A. J. Lazzarini, Nucl. Instrum. Methods 119, 145 (1974).

[12]L. C. Northcliffe and R. F. Schilling, Nucl. Data A7, (1970).

[13]C. W. Williams, W. E. Kiker and H. W. Schmitt, Rev. Sci. Instrum. 35, 1116 (1964).

[14]H. W. Schmitt, W. M. Gibson, J. H. Neiler, F. J. Walter, and T. D. Thomas, in *Proceedings of the First Symposium on the Physics and Chemistry of Fission, Salzburg, 1965* (International Atomic Energy Agency, Vienna, 1965), Vol. I.

[15]R. L. Kozub, N. H. Lu, J. M. Miller, D. Logan, T. W. Debiak, and L. Kowalski, Phys. Rev. C 11, 1497 (1975).

[16]E. Gadioli and L. Zetta, Phys. Rev. 167, 1016 (1968).

[17]P. J. Siemens, J. P. Bondorf, D. H. E. Gross, and F. Dickman, Phys. Lett. 36B, 24 (1971).

[18]J. Wilczynski, Phys. Lett. 47B, 484 (1973).

[19]J. S. Blair, Phys. Rev. 95, 1218 (1954).

[20]W. E. Frahn, Phys. Rev. Lett. 26, 358 (1971); Ann. Phys. (N.Y.) 72, 524 (1972).

[21]D. H. E. Gross and H. Kalinowski, Phys. Lett. 48B, 302 (1974).

[22]F. Plasil and M. Blann, Phys. Rev. C 11, 508 (1975).

[23]F. Puhlhofer and R. M. Diamond, Nucl. Phys. A191, 561 (1972).

[24]R. Vandenbosch and J. R. Huizenga, *Nuclear Fission* (Academic, New York, 1973).